Different Metabolic Responses in α-, β-, and δ-Cells of the Islet of Langerhans Monitored by Redox Confocal Microscopy

Ivan Quesada, Mariana G. Todorova, and Bernat Soria
Institute of Bioengineering, Miguel Hernandez University, Sant Joan d' Alacant, Spain

ABSTRACT   Blood glucose homeostasis is mainly achieved by the coordinated function of pancreatic α-, β-, and δ-cells, which secrete glucagon, insulin, and somatostatin, respectively. Each cell type responds to glucose changes with different secretion patterns. Currently, considerable information can be found about the signal transduction mechanisms that lead to glucose-mediated insulin release in the pancreatic β-cell, mitochondrial activation being an essential step. Increases in glucose stimulate the mitochondrial metabolism, activating the tricarboxylic acid cycle and raising the source of redox electron carrier molecules needed for respiratory ATP synthesis. However, little is known about the glucose-induced mitochondrial response of non-β-cells and its role in the stimulus-secretion coupling process. This limited information is probably a result of the scarcity of these cells in the islet, the lack of identification patterns, and the technical limitations of conventional methods. In this study, we used flavin adenine dinucleotide redox confocal microscopy as a noninvasive technique to specifically monitor mitochondrial redox responses in immunoidentified α-, β-, and δ-cells in freshly isolated intact islets and in dispersed cultured cells. We have shown that glucose provokes metabolic changes in β- and δ-cell populations in a dose-dependent manner. Conversely, no significant responses were observed in α-cells, despite the sensitivity of their metabolism to drugs acting on the mitochondrial function, and their intact ability to develop Ca^{2+} signals. Identical results were obtained in islets and in cultures of dispersed cells. Our findings indicate metabolic differences in glucose utilization among the α-, β-, and δ-cell populations, which might be important in the signal transduction events that lead to hormone release.

INTRODUCTION

The islet of Langerhans is the main endocrine unit controlling glucose homeostasis (1,2). Its function is the result of the interaction and secretion of many glucose-sensitive cell types, including β (60–80% of islet cells), α (10–15%), and δ-cells (5–10%), among others (1,3,4). Whereas α-cells release the hyperglycemic hormone glucagon when extracellular glucose concentrations become low, pancreatic β-cells secrete insulin in response to high concentrations of sugar to restore normal levels (1,3–5). Thus, the antagonist action of both hormones ensures glycemia within a physiological range. Additionally, somatostatin-containing δ-cells affect glucose homeostasis through the paracrine modulation of the neighboring α- and β-cells (6–8). Failures in this system may lead to the widespread disease diabetes mellitus (2). Despite the importance of non-β-cells for the whole islet function, the vast majority of studies have been focused on the β-cell physiology.

This insufficient knowledge about non-β-cells is partly due to both the scarcity of these cell types in the islet, and the lack of identification patterns. Additionally, it has been proved that the use of conventional techniques to monitor physiological parameters of non-β-cells in the intact islet is difficult and, to some extent, unsuccessful. Recently, some groups, as well as ours, have characterized the individual electrophysiological properties and Ca^{2+} signals in response to glucose of the main cell types in the intact islet of Langerhans (4,9–11). These studies have also demonstrated the existence of differences in the physiological behavior when data from dispersed cultured islet cells and fresh intact islets are compared. Undoubtedly, the latter is the model whose behavior is closer to the physiological scenario (12,13). Although these studies have contributed important physiological information, the data about the signal transduction pathway that leads to secretion in non-β-cells is still scarce, especially concerning events involved in cell metabolism.

In the case of the pancreatic β-cell, extracellular glucose is carried through membrane transporters into the cytosol, where it is then metabolized into pyruvate by glycolysis (14). Pyruvate enters the mitochondria and is further metabolized via the tricarboxylic acid (TCA) cycle, producing CO_2 and the nucleotide carriers of reducing power, NADH and $FADH_2$ (14–18). These molecules serve as a source of electron transfer in the chain of oxidative phosphorylation reactions that mediate ATP production. The increase in the ATP/ADP ratio is the main cause for the closure of ATP-dependent K^+ (K_{ATP}) channels, which leads to membrane depolarization and the increase in cytosolic $[Ca^{2+}]$ through the activation of voltage-dependent Ca^{2+} channels (2,19–21). This Ca^{2+} signal triggers insulin secretion. Although cytosolic glycolysis is coupled to a limited production of ATP and NADH, the major source of ATP and redox molecules comes from the oxidative mitochondrial metabolism (14,17). Thus, mitochondrial activation is a crucial step in the

signal-transduction events that lead to ATP-dependent insulin release in the pancreatic β-cell (14,17).

Most of the information about islet metabolism comes from biochemical studies. Notwithstanding the importance of this classical methodology, optical techniques combined with imaging have unique advantages to study the temporal and spatial pattern of different physiological parameters. Particularly, redox microfluorometry has been used as a non-invasive tool to monitor islet metabolism. The basis of this technique counts on the fluorescence properties of both NAD^+- and $NADP^+$ $(NAD(P)^+)$- and flavin adenine dinucleotide (FAD)-linked proteins (flavoproteins) and their associated intensity changes, depending on the cellular metabolic redox state (22). Whereas fluorescence is increased with the reduction of $NAD(P)^+$ into $NAD(P)H$, in the case of flavoproteins, the fluorescence intensity is higher for the oxidized form (FAD), and lower for the reduced molecule ($FADH_2$). Thus, these two molecules produce opposite fluorescence profiles when a change in the metabolic status takes place. Since $NAD(P)H$ is produced by glycolysis and the TCA cycle, the fluorescence signal comes from both compartments, the cytosol and the mitochondria (22). Conversely, the changes in flavoprotein fluorescence provide a better approach to monitor mitochondrial activation, since the reduction of these molecules occurs at the level of this intracellular organelle. However, although this methodology has been successful to investigate β-cell metabolism (16), redox fluorometry combined with conventional microscopy is not useful to spatially and temporally resolve the metabolic signal from non-β-cells in the intact islet. Indeed, this technique essentially detects the average signal, which is dominated by the most abundant population, the β-cell (4). This limitation can be mostly overcome using optical sectioning techniques. In this study, we have monitored FAD fluorescence signals using confocal microscopy to study the mitochondrial responses from individual α-, β-, and δ-cells in the intact islet of Langerhans and in dispersed cells in culture. Important metabolic differences in response to glucose are shown among the main islet cell types. These observations suggest important discrepancies about the stimulus-secretion coupling scheme of islet cells, especially when metabolic events are considered.

MATERIALS AND METHODS

Islet and cell isolation

All experiments were conducted according to regulations approved by our institution. Swiss albino OF1 mice (8–10 weeks old) were sacrificed by cervical dislocation, and pancreatic islets were then isolated by collagenase digestion as previously described (11,23). Intact islets were placed in a cell-culture chamber at 37°C for 30 min before the experiments. Some islets were dispersed into single cells and clusters by enzymatic digestion in the presence of 0.05% trypsin and 0.02% EDTA for 2 min. Cells and clusters were plated onto poly-L-lysine-treated coverslips and cultured overnight in RPMI 1640 (Invitrogen, Barcelona, Spain) supplemented with 10% fetal calf

serum, 100 IU/ml penicillin, 0.1 mg/ml streptomycin, and 5.6 mmol/L glucose (11,23). All experiments were carried out at 37°C.

Redox confocal microscopy

Intact islets were allowed to become attached onto poly-L-lysine-treated coverslips for 10 min before experiments. Islets or dispersed cells were then placed on a perfusion chamber mounted on the stage of a Zeiss LSM 510 laser confocal microscope system, and perfused at a rate of 1 ml/min in a Krebs-Ringer buffer (in mmol/L): 115 NaCl, 5 KCl, 10 $NaHCO_3$, 1.2 KH_2PO_4, 1.1 $MgCl_2$, 2.5 $CaCl_2$, 25 HEPES, and different concentrations of glucose (pH 7.4). Fluorescence was monitored using a $40\times$ oil immersion objective (numerical aperture 1.3). Confocal configuration was set to obtain optical sections of 6–8 μm and to optimize the capture of fluorescence changes from the FAD-linked proteins of our samples. Flavoprotein autofluorescence was excited at 488 nm with an argon laser, and the emission was collected with a bandpass at 505–550 nm. Two or four images were averaged for each acquisition point (1 point/2 s or 1 point/4 s). Temporal series were filtered with a spatial low-pass filter and processed using the digital image software of the Zeiss LSM 510 confocal microscope. The output of the 15-mW laser was adjusted around the minimum intensity (3%). The majority of experiments lasted >50 min. For these experiments, the interval time between each acquisition was set to 30–60 s. This sampling rate and laser intensity provided enough spatial resolution with a negligible photobleaching. For some shorter experiments the interval time was 5 s. Higher laser intensities improved the quality of the autofluorescence images but increased photobleaching (Fig. 1). Background was calculated by measuring fluorescence in a cell-free area of interest, and it was then subtracted from the records.

Immunocytochemistry

Once flavoprotein fluorescence changes had been recorded, intact islets or dispersed cells were washed for 10 min with phosphate-buffered saline, fixed using 1% (w/v) paraformaldehyde for 10 min, and permeabilized with 0.5% Triton X-100 for 10 min, as previously described (4,11) . To reduce nonspecific antibody binding, cells were first preincubated with a blocking buffer (2% goat serum in phosphate-buffered saline) for 15 min at room temperature before primary antibodies were applied in the same buffer. An antiinsulin monoclonal antibody (1:1000 dilution; Sigma, Barcelona, Spain), an antiglucagon monoclonal antibody (1:1000 dilution; Sigma), or an anti-somatostatin rabbit polyclonal antibody (1:300 dilution, Dakocytomation,
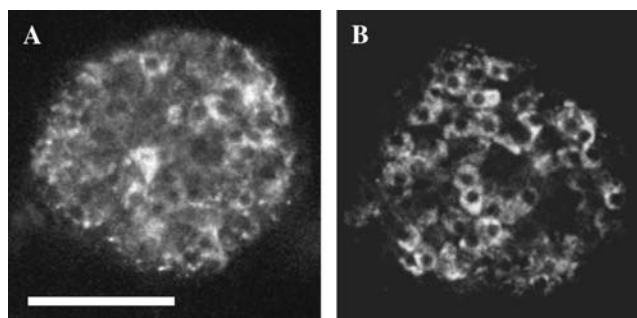

FIGURE 1 Autofluorescence in intact islets. Images of the fluorescence emission of two islets excited with a 15-mW argon laser at 488 nm. Emission was collected with a bandpass filter at 505–550 nm. The laser intensity was adjusted to 3% in the case of the islet shown in A, and at 10% in B. A laser intensity of 3% allowed temporal series of well-contrasted images without detectable photobleaching (please see Materials and Methods). Optical section, 6 μm; scale bar, 100 μm.

Barcelona, Spain) was applied for 3 h. After washing, fluorescein-isothiocyanate- or tetramethyl-rhodamine-isothiocyanate-conjugated secondary antibodies were applied for 2 h to visualize staining: a goat antimouse antibody (1:64 dilution; Sigma) was used for insulin or glucagon and a goat antirabbit antibody (1:64 dilution, Sigma) for somatostatin. Fluorescence was visualized using the same confocal system. In the case of the immunocytochemistry in intact islets, the same optical section was maintained as previously described (4). During all the inmmunochemistry, the preparation was continuously monitored by acquiring images (1 image/min) in the transmitted-light channel of the confocal microscope with a different wavelength from that used for immunodetection. Additionally, to avoid any movement of the sample derived from manipulation, we applied all the elements of the immunocytochemistry with the perfusion system at a very low rate flux. Because of the preparation's thickness, it is difficult for antibodies to stain the center of the whole islets, as has been previously reported (4,9,11). However, this is not a limitation for our experiments, given that the outer cell layers surrounding the center are represented by all the cell types that form the islet (4,9,11).

Cell viability test

After autofluorescence was recorded, the viability of the cells was tested in separate samples by loading them with 1 μM ethidium homodimer-1 and 2 μM calcein/acetoxymethyl ester (AM) (Molecular Probes, Madrid, Spain) for 15 min. Ethidium only stains the nucleus of cells whose plasma membrane integrity is compromised. Calcein/AM is a nonfluorescent probe that diffuses into the cell interior, where cytosolic esterases cleave it to produce a fluorescent product that is retained in the cytosol. Thus, living cells become green if their plasma membrane and enzymatic capacity remain intact. These probes were visualized with standard rhodamine and fluorescein configurations, respectively.

Ca^{2+} imaging

Cells were loaded with 4 μM Fluo-3/AM (20 min, 37°C) (Molecular Probes) in some samples, after FAD fluorescence was recorded. Cells were then washed with the extracellular medium to eliminate the circulating dye, and stimulated with 5 μM of adrenaline, which has been proved to specifically induce Ca^{2+} signals in α-cells (24,25). Cytosolic Ca^{2+} changes were monitored under the same confocal microscope at a rate of 1 image every 2–4 s. The Ca^{2+} probe was excited with the laser beam at 488 nm, and fluorescence was collected with a bandpass filter at 505–530 nm.

Statistical analysis and data representation

Fluorescence records were represented as the percentage of $\Delta F/F_0$ where F_0 is the fluorescence signal at the beginning of a record and ΔF is $F - F_0$. Student's t-test ($p < 0.05$) was performed with commercial software (SigmaPlot, Jandel, San Rafael, CA). Some data is shown as mean ± SE.

RESULTS

Glucose-induced metabolic changes in pancreatic β-cells in the intact islet

Redox fluorescence microscopy has been employed as a noninvasive technique to evaluate the involvement of metabolism activation in the signal transduction cascade that leads to insulin release in the pancreatic β-cell (16,18). Nevertheless, conventional optical techniques have several limitations to spatially and temporally resolve physiological variables in non-β-cells, especially when they are in the intact islet of Langerhans. These classical methods are mainly hindered by the out-of-focus information coming out from adjacent points other than those located in the focal plane. This is particularly noteworthy in the case of the islet of Langerhans, where a minority of non-β-cells are scattered throughout a cellular network mostly dominated by the pancreatic β-cell population. Consequently, signals coming from the former cells are masked by the β-cell-dominated average signal (4,11). However, problems derived from out-of-focus information are almost entirely eliminated by optical sectioning methods (Fig. 1).

In Fig. 2 we show an 8-μm optical slice of an intact islet of Langerhans and the temporal change of flavoprotein fluorescence in response to glucose. By increasing glucose concentrations there was a corresponding dose-dependent decrease in fluorescence as a result of FAD reduction (Fig. 2 B). NAD(P)H fluorescence is initiated in both compartments: a small fraction comes from cytosol because of glycolysis, whereas a main component arises from the mitochondria due to the TCA cycle activation (22,26). In contrast, flavoprotein signals only come from the mitochondrial compartment (14,17,22,27). Thus, glucose-induced changes in Fig. 2 essentially reflect graded responses of mitochondrial activation. Because oxidative phosphorylation is highly dependent on the mitochondrial redox potential, these fluorescence changes are likely to be coupled to increases in respiratory ATP synthesis, which are critical in ATP-dependent insulin secretion (22,27). Consistent with this idea, the mitochondrial uncoupler carbonyl cyanide p-trifluoromethoxyphenylhydrazone (FCCP) and the cytochrome oxidase inhibitor cyanide, which are expected to cause maximal levels of oxidation and reduction, respectively, produced the corresponding changes in fluorescence (Fig. 2 B). The protonophore effect of FCCP is responsible for the collapse of the mitochondrial membrane potential, leading to an increase in the respiratory rate, and thus promoting the oxidation of FADH$_2$ to FAD (28). In contrast, the electron chain inhibitor cyanide is expected to diminish the oxidation of reducing equivalents, producing an accumulation of the reduced forms (28). Four records measured from different positions within the islet optical section are shown along with the islet average signal, indicating a high degree of metabolic homogeneity. This average signal mimics, to some extent, what would be obtained with conventional optical techniques, which mainly capture the β-cell-dominated signal. We did not observe oscillations of the FAD signal when islets were challenged with glucose, as has been reported in some cases for the NAD(P)H fluorescence in cells of rat islets (14).

The typical metabolic pattern shown in Fig. 2 corresponds to the pancreatic β-cell population as confirmed by immunocytochemistry applied subsequently to the fluorescence record and image analysis of the same optical slice (Fig. 3). However, such a pattern and homogeneity is not as apparent if we analyze fluorescence changes individually in the intact islet.
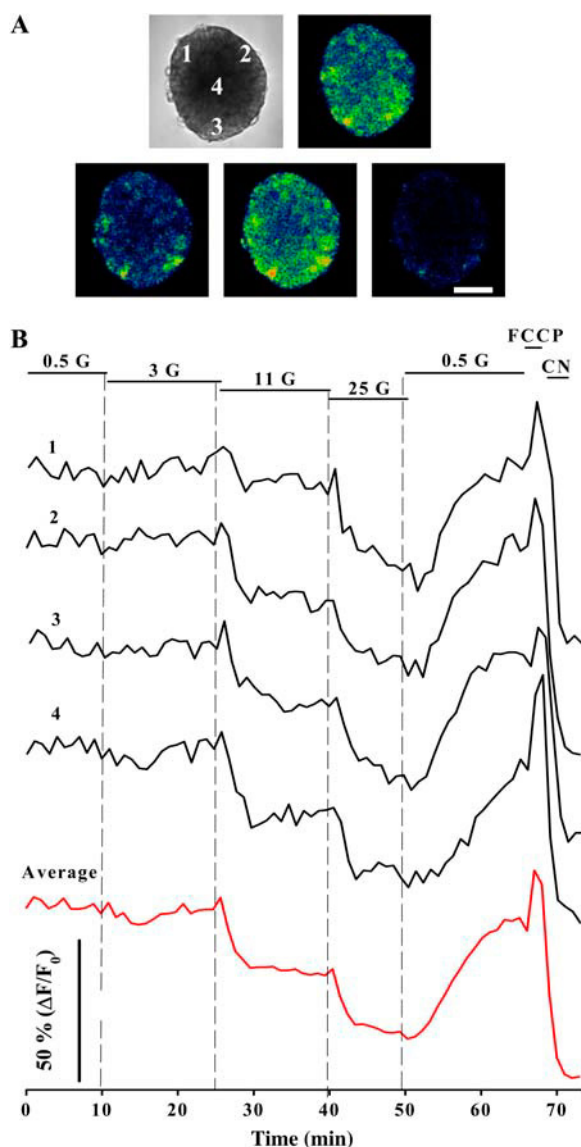
FIGURE 2   FAD fluorescence changes in response to glucose monitored in the intact islet of Langerhans. (*A*) Transmitted-light image of an islet and confocal images of FAD fluorescence in the presence of 3 mM glucose (*G*), 25 mM glucose, 10 μM FCCP, and 2 mM CN (*top left* to *bottom right*). Optical section, 8 μm; scale bar, 100 μm. Areas from which fluorescence changes are represented in *B* are also indicated. (*B*) Changes in fluorescence from four different areas of $20 \times 20 \ \mu$m are plotted as the percentage of $(F - F_0)/F_0$, where F_0 is the fluorescence at the beginning of the record. Red line shows the average fluorescence from the whole optical section of the islet selected for these measurements. These results are representative of nine islets. Glucose concentrations are given in millimolars. FCCP and CN were applied at 10 μM and 2 mM, respectively.

Fluorescence changes in response to glucose in α- and δ-cells

After acquiring FAD fluorescence changes in response to glucose in the intact islet, we performed immunocytochemistry using antiglucagon antibodies to identify α-cells in the same optical section (Fig. 4, *A* and *B*). We observed no
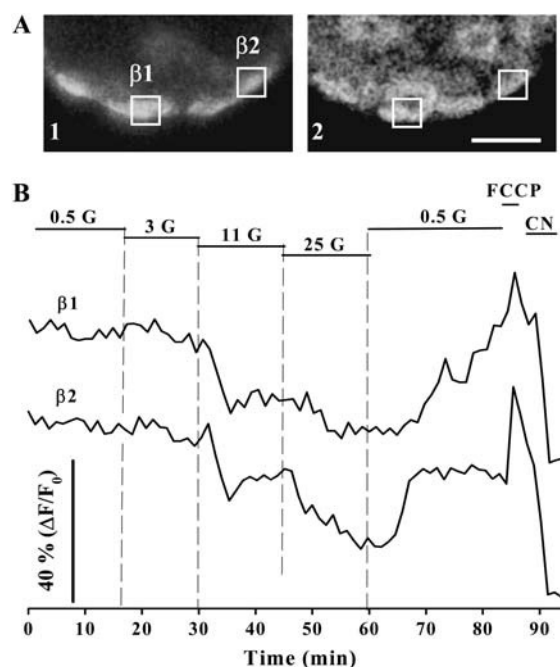

FIGURE 3   Metabolic changes in response to glucose in immunoidentified pancreatic β-cells. (*A*) Once fluorescence records were acquired, the islets were treated with antiinsulin antibodies to identify pancreatic β-cells. The images show the immunofluorescence (*1*) for the same optical section selected for the autofluorescence (*2*) record. Scale bar, 20 μm. (*B*) Fluorescence changes from two immunoidentified β-cells referred to as β1 and β2 are shown. The position of these cells is also indicated in *A*. Glucose concentrations are given in millimolars. FCCP and CN were applied at 10 μM and 2 mM, respectively.

evident effect when these cells were challenged with glucose, regardless of the concentration applied. FCCP and cyanide (CN) produced the expected fluorescence changes in α-cells, indicating both the integrity and responsiveness of the mitochondrial metabolism, and that this optical technique was not failing to detect FAD changes in these cells (Fig. 4 *B*). To further confirm the viability of α-cells during redox confocal measurements, we conducted additional experiments in dispersed cultured cells (Fig. 4 *C*). First, we incubated cells with calcein/AM and ethidium homodimer-1 in separate samples (see Materials and Methods), after acquiring FAD fluorescence as shown in Fig. 4 *B*. All the immunoidentified α-cells tested had a response similar to the one shown in Fig. 4 *B* and retained their enzymatic activity and plasma membrane integrity (not shown; $n = 12$ cells from three experiments). Second, after FAD records, cells were loaded for 20 min with the fluorescent Ca^{2+} reporter Fluo-3 (Fig. 4 *D*). Then, the cells were exposed to adrenaline, which has been proved to induce Ca^{2+} signals in α-cells, probably by Ca^{2+} mobilization from intracellular stores (25). Fig. 4 *D* illustrates a typical adrenaline-induced Ca^{2+} response after monitoring FAD fluorescence changes in two immunoidentified α-cells, demonstrating the integrity of the signaling system to induce cytosolic Ca^{2+} elevations. Thus,
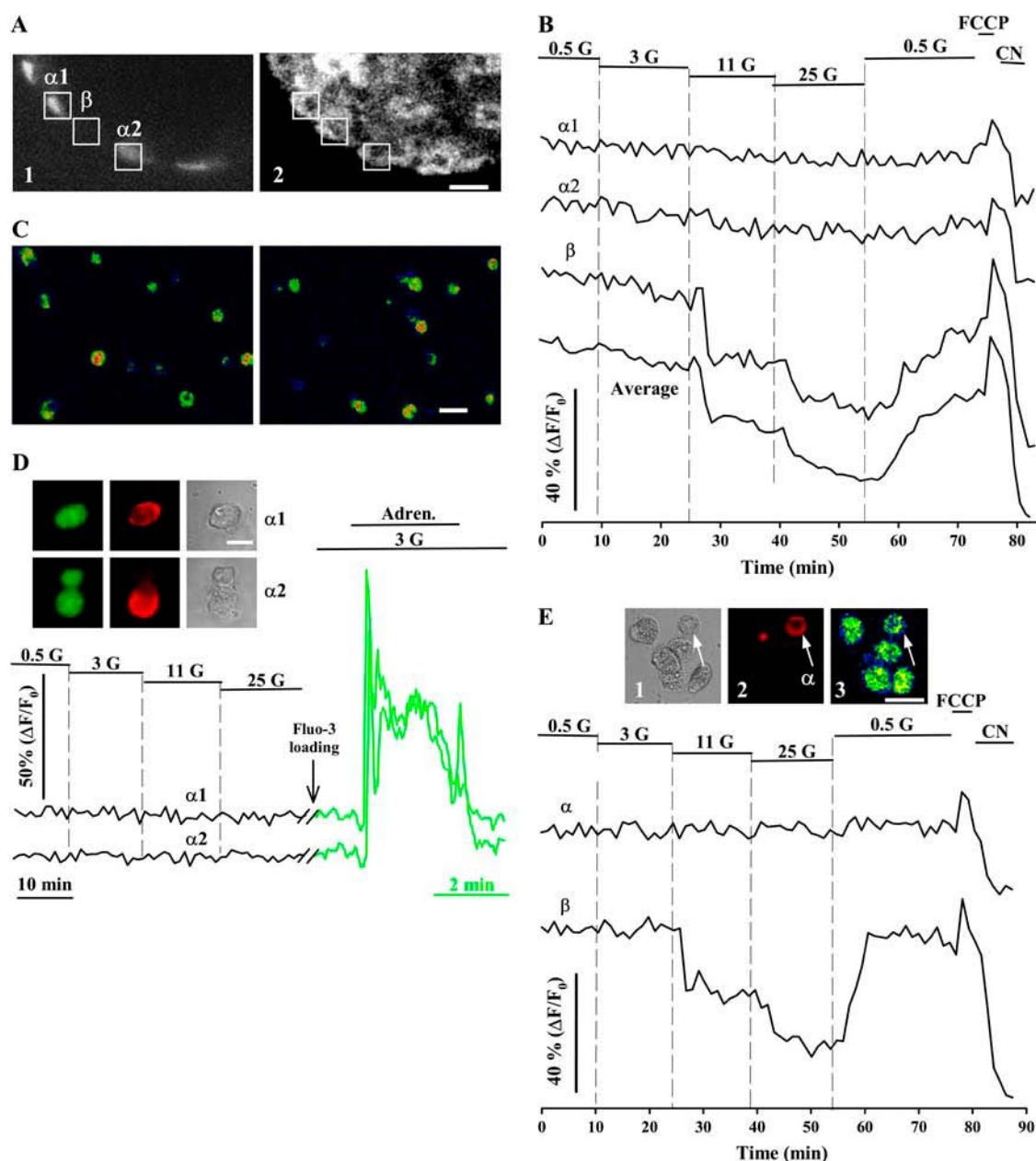
FIGURE 4 Glucose-induced metabolic responses in pancreatic α-cells. (A) Subsequent to fluorescence records, an immunocytochemistry with antiglucagon antibodies was performed to identify pancreatic α-cells in the intact islet. The images show the immunofluorescence (1) for the same optical section selected for the autofluorescence (2) record. Scale bar, 15 μm. (B) Fluorescence changes in response to glucose of two immunoidentified α-cells (α1 and α2). A typical β-cell record and the average signal from the whole optical section of this islet are also shown for comparison. The position of cells (α1 and α2) is indicated in A. (C) Two different fields showing the autofluorescence of dispersed islet cells. Scale bar, 30 μm. (D) In separate experiments, cells were loaded for 20 min with Fluo-3, a fluorescent Ca^{2+} reporter, after acquiring FAD fluorescence changes. Adrenaline (Adren.), which has been proved to induce Ca^{2+} signals in α-cells, was applied to the bath at 5 μM. Redox-associated fluorescence changes (black line) and adrenaline-induced Ca^{2+} signals (green line) from two immunoidentified α-cells (α1 and α2) are shown in the figure. These records represent the findings of seven different experiments. The images illustrate the incorporation of Fluo-3 in these two cells (green) and the immunofluorescence with antibodies against glucagon (red) along with the transmitted-light image of the same field after chemical fixation. A cell not positive for antiglucagon antibodies is also shown next to α2. Scale bar, 10 μm. (E) Glucose-induced responses of dispersed islet cells in culture. Records illustrate the typical patterns of immunoidentified pancreatic α- and β-cells. In all the experiments, glucose concentrations are given in millimolars. FCCP and CN were applied at 10 μM and 2 mM, respectively. The transmitted-light (1) and fluorescence (2) images on the top illustrate the immunoidentification of the α-cell whose record is shown in this figure. An image of the autofluorescence of these cells is also shown (3). Scale bar, 20 μm.

several lines of evidence confirm that the viability of α-cells was not compromised during FAD measurements.

Once more, the islet average signal along the optical section shows that it is indeed dominated by the β-cell metabolic pattern (Fig. 4 B), resembling, to some extent, a situation that would be obtained with conventional optical techniques (4,18). These results further indicate that conventional microscopy is not suitable to resolve metabolic signals from non-β-cells in the islet. The quantification of the fluorescence signals in response to glucose of α-cells within the islet revealed a very small effect with 11 mM of glucose ($\sim$4%) (see Fig. 6 A). Because cells are densely packed into the islet, image analysis of the regions of interest became occasionally difficult to establish cell boundaries. To avoid any potential contribution from neighboring adjacent β-cells to the fluorescence signal coming from α-cells, we performed similar experiments in isolated cells cultured overnight. Fig. 4 E shows a typical record from immunoidentified α- and β-cells. In these conditions, the response of α-cells to high concentrations of glucose was <2% (see Fig. 6 B), indicating that there probably exists a small contribution from the β-cell signal in intact islets in the analysis shown in

Fig. 5 A. In some experiments, fluorescence was recorded every 5–10 s for 10 min when glucose was changed from 0.5 to 25 mM, giving similar results ($n = 5$, not shown). Since the availability of redox molecules affects oxidative phosphorylation (14,22,27), this minimal response of FAD fluorescence in α-cells is indicative of low respiratory ATP synthesis in the presence of glucose. Thus, altogether, these observations point to a limited involvement of the mitochondrial metabolism in the α-cell signal transduction scheme in response to glucose.

The effect of glucose on the mitochondrial metabolism was also monitored in immunoidentified pancreatic δ-cells in both fresh intact islets (Fig. 5, A and B) and isolated cells in culture (Fig. 5 C). Identical results were obtained in both approaches (Figs. 5 and 6). Glucose increased the mitochondrial redox potential in a dose-dependent manner. Fluorescence changes in δ-cells were, in all cases, smaller than signals from pancreatic β-cells, probably reflecting the special metabolic configuration of the latter cells for oxidative glucose metabolism in the mitochondria (29,30).

To further demonstrate these particular metabolic patterns, we also monitored the signal changes derived from NAD(P)H
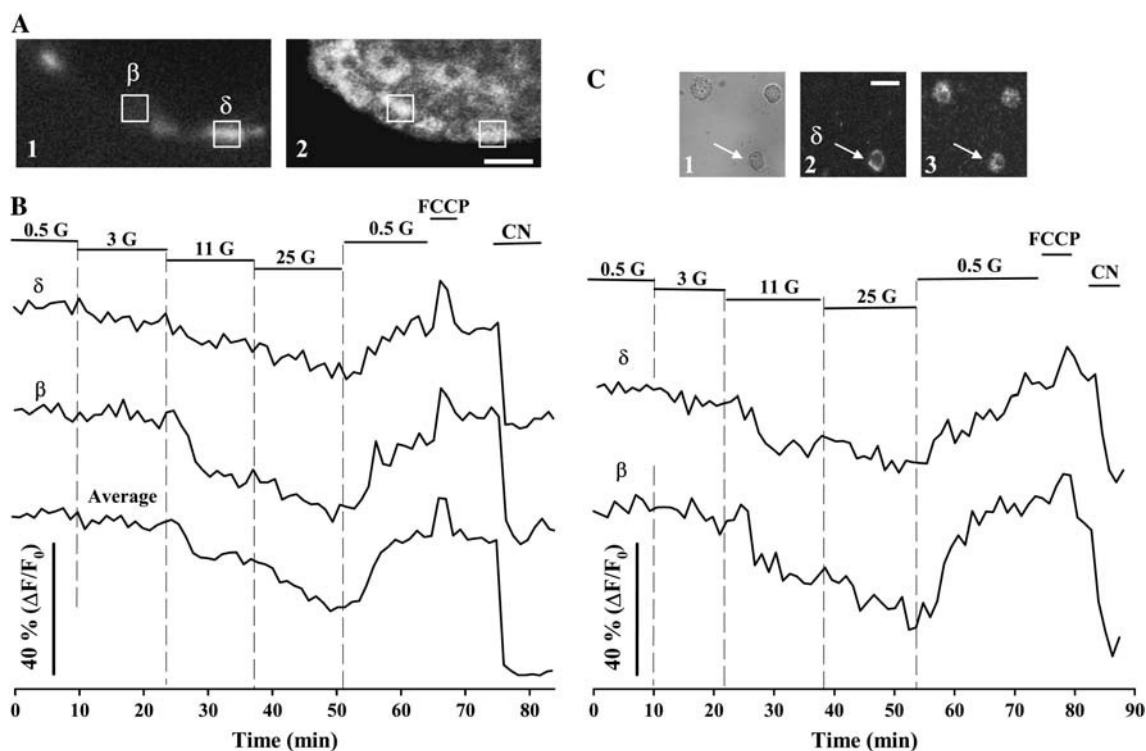

FIGURE 5 Glucose-induced metabolic responses in pancreatic δ-cells. (A) Once measurements of autofluorescence were performed, pancreatic δ-cells were identified by means of an immunocytochemistry with antisomatostatin antibodies. The image shows the immunofluorescence for the same optical slice selected for FAD fluorescence records. Scale bar, 15 μm. (B) Changes in fluorescence in response to glucose of an immunoidentified δ-cell. A typical β-cell record and the average signal from the islet whole optical section are also shown for comparison. The position of the represented cells is indicated in A. (C) Evolution of FAD fluorescence in dispersed islet cells in culture. These records illustrate the typical patterns of immunoidentified pancreatic δ- and β-cells. Glucose concentrations are given in millimolars.. FCCP and CN were applied at 10 μM and 2 mM, respectively. The transmitted-light (1) and fluorescence (2) images on the top illustrate the immunoidentification of the δ-cell whose record is shown in this figure. An image of the autofluorescence of these cells is also shown (3). Scale bar, 15 μm.
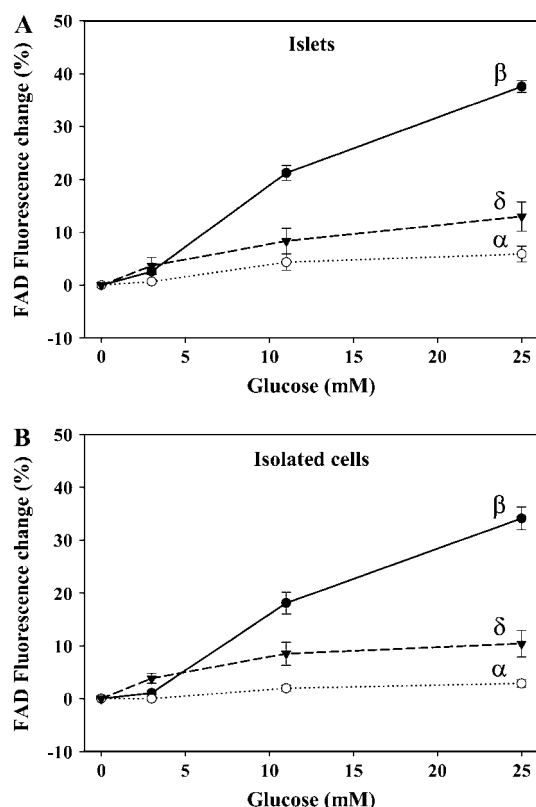
FIGURE 6   Percentage of FAD fluorescence change of each cell type in the intact islet (*A*) and in culture (*B*). The percentage was calculated as the change in fluorescence from the signal obtained with 0.5 mM glucose. Results are shown as the mean $\pm$ SE from 19 β-cells (three islets), 9 α-cells (four islets), and 7 δ-cells (four islets) and from 45 β-cells (nine cultures), 36 α-cells (six cultures), and 13 δ-cells (four cultures). All values were found to be significant except the fluorescence change obtained in α-cells with 3 mM glucose ($p < 0.05$, compared with basal values).

autofluorescence using conventional microscopy and dispersed cells (see figure in Supplementary Material.). The pattern of the NAD(P)H signal in the presence of glucose, FCCP, and CN was inverse to the one obtained for the FAD fluorescence, since these two molecules generate opposite fluorescence profiles when a change in the metabolic status takes place (16,22,27,28). The analysis of the NAD(P)H fluorescence is more complicated: a small fraction comes from the cytosol because of glycolysis, whereas a main component arises from the mitochondrial activation (22,28). Nevertheless, the results obtained with NAD(P)H fluorescence pointed to a particular metabolic response in each cell type, which was very similar to the pattern found with FAD measurements.

DISCUSSION

In this study, we have used redox confocal microscopy to monitor the mitochondrial metabolic changes in response to glucose of unambiguously identified α-, β-, and δ-cells in

fresh intact islets and dispersed in culture. So far, specific studies addressing the physiological behavior of non-β-cells are not abundant, despite the importance of these cell types for the physiology and pathophysiology of the islet of Langerhans (3,31). Existing information about non-β-cells is even more infrequent when considering reports dealing with fresh intact islets, a preparation closer to the physiological situation, as evidenced by in vivo studies (12,13). Although biochemical investigations have certainly provided important data using cell purification protocols, which are not always free from partial contamination, these methods fail to spatially and temporally track cellular variables in individual islet cells (32–35). Conventional optical and imaging techniques present intrinsic difficulties for resolving non-β-cells in the intact islet because of the limitations derived from the out-of-focus information, along with the scarcity of these cell types. Alternatively, as we have shown in this study and in previous reports, optical-sectioning methods are valuable tools for monitoring cellular parameters from individual cells in intact islets (4,11). This is particularly noteworthy to track non-β-cell physiology. Besides the important limitation imposed by the minor representation of non-β-cells in the islet, another major drawback to investigating these cells is the lack of identification patterns. In addition to the electrophysiological and Ca^{2+}-signaling typical patterns previously reported (4,9,10,36), our observations in this study allow for another physiological criterion, based on characteristic metabolic responses, to identify these cells in the intact islet of Langerhans.

Some studies addressing β-cell metabolism have measured NAD(P)H fluorescence changes. This maneuver, however, entails some analysis complications since the NAD(P)H signal does not allow cytosolic glycolysis and mitochondrial metabolism to be distinguished (22,26,27). Although some efforts have been made to spatially resolve NAD(P)H signal from both cell compartments, these experimental procedures involved the culture of islets for several days on an extracellular matrix to allow them to spread out (26,37). This situation may dramatically differ from physiological behavior, given that studies with islets cultured for long times indicate important differences (12,13,38,39). However, the FAD fluorescence signal originates from the mitochondria and is used as an intracellular probe of the mitochondrial metabolic state and the respiratory ATP synthesis in many cell types (22,27,40). In the pancreatic β-cell, mitochondrial activation is a key event in the current signaling model for glucose-mediated insulin secretion (14). Glucose metabolism modifies the cellular redox state, increasing the concentration of nucleotide carriers of reducing power, NAD(P)H and $FADH_2$, which participate in the electron transport chain and, thereby, facilitate ATP production by oxidative phosphorylation (14,16,17,41). The resulting increase in the ATP/ADP ratio is responsible for K_{ATP} channel inhibition and the depolarization-induced Ca^{2+} increase that precedes exocytosis (2,21). All these metabolic and ionic changes lead to insulin secretion.

However, the model for glucose-induced signal transduction in α-cells is still a matter of debate at this time. The stimulation of glucagon secretion depends on multiple levels of control, including low glucose concentrations, amino acids, and hormonal and neuronal inputs, whose dominance varies depending on the physiological situation (7,42–44). Notwithstanding the significance of all these regulatory factors, glucose exerts a significant control on the α-cell function (10,24,33,45). Several studies have contributed important data regarding the glucose dependence of the α-cell response, showing its opposite behavior compared to β-cells in terms of electrical activity, Ca^{2+} signaling, and secretion when glucose levels are increased (4,10,11,36,45). Recently, several reports have specifically demonstrated a direct effect of glucose on α-cell glucagon secretion, independent of other factors (24,46). Many significant features in α-cells, such as the existence of K_{ATP} channels, glucose-dependent electrical activity, and Ca^{2+} signals, as well as Ca^{2+}-induced exocytosis, have made it possible to propose a model to explain glucose regulation of glucagon release mainly based on ionic events (10,47). As proposed for β-cells, it has been hypothesized that glucose metabolism may be a critical link that couples these electrical and Ca^{2+} changes with glucagon secretion (10,47). However, glucose-induced metabolic variations and the activation of the mitochondrial function have not been explored in unambiguously identified α-cells. Our observations indicate that, contrary to the situation for β-cells, mitochondrial oxidative metabolism is not a major step in the glucose-mediated signaling pathway for the regulation of glucagon release in α-cells. Thus, other metabolic processes might have a primary role. In this aspect, our results are in agreement with biochemical studies using purification protocols or lines derived from islet cell types that have reported the existence of metabolic differences between islet cells. It is worth mentioning that adenine nucleotide changes in response to glucose occur in β- but not in α-cells, suggesting a high degree of coupling between cytosolic glycolysis and mitochondrial respiratory ATP synthesis in the former cell type that would not take place in α-cells (32). Actually, related biochemical studies point to a prevalence of anaerobic glycolysis in non-β-cells (most likely purified α-cells) as opposed to an aerobic metabolism in β-cells (48). This idea is also supported by the finding that the ratio lactate dehydrogenase/mitochondrial glycerol phosphate dehydrogenase is low in β-cells, which would favor mitochondrial oxidation, but elevated in non-β-cells (29). It is unlikely that this limited involvement of the α-cell mitochondria in glucose metabolism is attributable to significant restrictions in upstream reactions involved in glucose utilization and/or uptake. In fact, although α- and β-cells possess different glucose transporters and kinetics for sugar incorporation, glucose transport is not rate-limiting because it exceeds glucose utilization by several times, the latter process being similar in both cell types (34,49,50). Given that glucose

metabolism also participates in many other cell processes other than glucagon secretion (51,52), our results in α-cells would also limit the involvement of the mitochondrial metabolism as a central element in other glucose-mediated signaling and energetic pathways.

The situation, however, is quite different for the δ-cell. Although information about glucose regulation of somatostatin secretion is also scarce, several physiological characteristics point to control mechanisms similar to those described for β-cells. Increasing glucose concentrations activates electrical activity, Ca^{2+} signals, and secretion, a situation analogous to the one occurring in β-cells, and opposed to the α-cell response (4,6,8,10,11,53). K_{ATP} channels are present in the δ-cell and their closure by sulphonylureas induces cytosolic Ca^{2+} elevations and somatostatin secretion (11,54). It has been suggested that, upon glucose stimulation, these metabolic regulated K^+ channels may link the metabolic redox state of the cell with changes of the membrane potential, which may lead to Ca^{2+} entry and somatostatin secretion (1,9). Therefore, it seems very likely that δ-cells have a stimulus-secretion coupling scheme very similar to the one established in the β-cell, as has been previously proposed (1,9). Our results in δ-cells agree with this signal transduction process. The data reported here indicate that glucose stimulates the activation of the mitochondrial oxidative metabolism and changes in the cellular redox state, probably fulfilling a function similar to the one in the β-cell. Our observations are also consistent with studies that emphasize the critical role of the glucose mitochondrial metabolism for other functions in δ-cells, such as gene expression (55). Although the stimulus-secretion coupling is well-understood in the pancreatic β-cell, further work is needed to fully understand the regulation of α- and δ-cells.

SUPPLEMENTARY MATERIAL

An online supplement to this article can be found by visiting BJ Online at http://www.biophysj.org.

REFERENCES

1. Kanno, T., S. O. Gopel, P. Rorsman, and M. Wakui. 2002. Cellular function in multicellular system for hormone-secretion: electrophysiological aspect of studies on α-, β- and δ-cells of the pancreatic islet. *Neurosci. Res.* 42:79–90.

2. Prentki, M., and F. M. Matchinsky. 1987. Ca^{2+}, cAMP and phospholipid-derived messengers in coupling mechanisms of insulin secretion. *Physiol. Rev.* 67:1185–1248.

3. Barg, S. 2003. Mechanisms of exocytosis in insulin-secreting β-cells and glucagon-secreting α-cells. *Pharmacol. Toxicol.* 92:3–13.

4. Nadal, A., I. Quesada, and B. Soria. 1999. Homologous and hetero-logous asynchronicity between identified α-, β- and δ-cells within intact islets of Langerhans in the mouse. *J. Physiol.* 517:85–93.

5. Sugino, F., T. Ishikawa, S. Nakada, Y. Kaneko, Y. Yamamoto, and K. Nakayama. 2002. Inhibition by nitric oxide of Ca^{2+} responses in rat pancreatic α-cells. *Life Sci.* 71:81–89.

6. Berts, A., A. Ball, S. Dryselius, E. Gylfe, and B. Hellman. 1996. Glucose stimulation of somatostatin-producing islet cells involves oscil-latory Ca^{2+} signaling. *Endocrinology.* 137:693–697.

7. Berts, A., A. Ball, E. Gylfe, and B. Hellman. 1996. Suppression of Ca^{2+} oscillations in glucagon-producing 2-cells by insulin/glucose and amino acids. *Biochim. Biophys. Acta.* 1310:212–216.

8. Berts, A., E. Gylfe, and B. Hellman. 1995. Ca^{2+} oscillations in pancreatic islet cells secreting glucagon and somatostatin. *Biochem. Biophys. Res. Commun.* 208:644–649.

9. Gopel, S. O., T. Kanno, S. Barg, and P. Rorsman. 2000. Patch-clamp characterisation of somatostatin-secreting δ-cells in intact mouse pancreatic islets. *J. Physiol.* 528:497–507.

10. Gopel, S. O., T. Kanno, S. Barg, X. G. Weng, J. Gromada, and P. Rorsman. 2000. Regulation of glucagon release in mouse α-cells by K_{ATP} channels and inactivation of TTX-sensitive Na^+ channels. *J. Physiol.* 528:509–520.

11. Quesada, I., A. Nadal, and B. Soria. 1999. Different effects of tolbutamide and diazoxide in α, β and δ cells within intact islets of Langerhans. *Diabetes.* 48:2390–2397.

12. Fernandez, J., and M. Valdeolmillos. 2000. Synchronous glucose-dependent $[Ca^{2+}]_i$ oscillations in mouse pancreatic islets of Langerhans recorded in vivo. *FEBS Lett.* 477:33–36.

13. Sanchez-Andres, J. V., A. Gomis, and M. Valdeolmillos. 1995. The electrical activity of mouse pancreatic β-cells recorded in vivo shows glucose-dependent oscillations. *J. Physiol.* 486:223–228.

14. Kennedy, E. D., and C. B. Wollheim. 1998. Role of mitochondrial calcium in metabolism-secretion coupling in nutrient-stimulated insulin release. *Diabetes Metab.* 24:15–24.

15. Bennett, B. D., T. L. Jetton, G. Ying, M. A. Magnuson, and D. W. Piston. 1996. Quantitative subcellular imaging of glucose metabolism within intact pancreatic islets. *J. Biol. Chem.* 271:3647–3651.

16. Civelek, V. N., J. T. Deeney, K. Kubik, V. Schultz, K. Tornheim, and B. E. Corkey. 1996. Temporal sequence of metabolic and ionic events in glucose-stimulated clonal pancreatic β-cells (HIT). *Biochem. J.* 315: 1015–1019.

17. Maechler, P., and C. B. Wollheim. 2001. Mitochondrial function in normal and diabetic β-cells. *Nature.* 414:807–812.

18. Pertusa, J. A., R. Nesher, N. Kaiser, E. Cerasi, J. C. Henquin, and J. C. Jonas. 2002. Increased glucose sensitivity of stimulus-secretion coupling in islets from *Psammomys obesus* after diet induction of diabetes. *Diabetes.* 51:2552–2560.

19. Ashcroft, F. M., D. E. Harrison, and S. J. Ashcroft. 1984. Glucose induces closure of single potassium channels in isolated rat pancreatic β-cells. *Nature.* 312:446–448.

20. Santos, R. M., L. M. Rosario, A. Nadal, J. Garcia-Sancho, B. Soria, and M. Valdeolmillos. 1991. Widespread synchronous $[Ca^{2+}]_i$ oscil-lations due to bursting electrical activity in single pancreatic islets. *Pflugers Arch.* 418:417–422.

21. Valdeolmillos, M., A. Nadal, D. Contreras, and B. Soria. 1992. The relationship between glucose-induced K_{ATP} channel closure and the rise in $[Ca^{2+}]_i$ in single mouse pancreatic islet cells. *J. Physiol.* 455: 173–186.

22. Masters, B. R., and B. Chance. 1993. Redox confocal imaging: intrinsic fluorescent probes of cellular metabolism. *In* Fluorescent and Luminescent Probes for Biological Activity. W. T. Mason, editor. Academic Press, London. 44–57.

23. Quesada, I., J. M. Rovira, F. Martin, E. Roche, A. Nadal, and B. Soria. 2002. Nuclear K_{ATP} channels trigger nuclear Ca^{2+} transients that modulate nuclear function. *Proc. Natl. Acad. Sci. USA.* 99:9544–9549.

24. Gromada, J., X. Ma, M. Hoy, K. Bokvist, A. Salehi, P. O. Berggren, and P. Rorsman. 2004. ATP-sensitive K^+ channel-dependent regula-tion of glucagon release and electrical activity by glucose in wild-type and SUR1$-/-$ mouse α-cells. *Diabetes.* 53:S181–S189.

25. Liu, Y. J., E. Vieira, and E. Gylfe. 2004. A store-operated mechanism determines the activity of the electrically excitable glucagon-secreting pancreatic α-cell. *Cell Calcium.* 35:357–365.

26. Patterson, G. H., S. M. Knobel, P. Arkhammar, O. Thastrup, and D. W. Piston. 2000. Separation of the glucose-stimulated cytoplasmic and mitochondrial NAD(P)H responses in pancreatic islet β cells. *Proc. Natl. Acad. Sci. USA.* 97:5203–5207.

27. Zima, A. V., J. Kockskamper, R. Mejia-Alvarez, and L. A. Blatter. 2003. Pyruvate modulates cardiac sarcoplasmic reticulum Ca^{2+} release in rats via mitochondria-dependent and -independent mechanisms. *J. Physiol.* 550:765–783.

28. Duchen, M. R. 1999. Contributions of mitochondria to animal physiology: from homeostatic sensor to calcium signalling and cell death. *J. Physiol.* 516:1–17.

29. Ainscow, E. K., C. Zhao, and G. A. Rutter. 2000. Acute over-expression of lactate dehydrogenase-A perturbs β-cell mitochondrial metabolism and insulin secretion. *Diabetes.* 49:1149–1155.

30. Sekine, N., V. Cirulli, R. Regazzi, L. J. Brown, E. Gine, J. Tamarit-Rodriguez, M. Girotti, S. Marie, M. J. MacDonald, C. B. Wollheim, and G. A. Rutter. 1994. Low lactate dehydrogenase and high mito-chondrial glycerol phosphate dehydrogenase in pancreatic β-cells. Potential role in nutrient sensing. *J. Biol. Chem.* 269:4895–4902.

31. Unger, R. H. 1985. Glucagon physiology and pathophysiology in the light of new advances. *Diabetologia.* 28:574–578.

32. Detimary, P., S. Dejonghe, Z. Ling, D. Pipeleers, F. Schuit, and J. C. Henquin. 1998. The changes in adenine nucleotides measured in glucose-stimulated rodent islets occur in β cells but not in α cells and are also observed in human islets. *J. Biol. Chem.* 273:33905–33908.

33. Gorus, F. K., W. J. Malaisse, and D. G. Pipeleers. 1984. Differences in glucose handling by pancreatic α- and β-cells. *J. Biol. Chem.* 259: 1196–1200.

34. Heimberg, H., A. De Vos, D. Pipeleers, B. Thorens, and F. Schuit. 1995. Differences in glucose transporter gene expression between rat pancreatic α- and β-cells are correlated to differences in glucose transport but not in glucose utilization. *J. Biol. Chem.* 270:8971–8975.

35. Pipeleers, D. G., P. A. In't Veld, M. Van de Winkel, E. Maes, F. C. Schuit, and W. Gepts. 1985. A new in vitro model for the study of pancreatic α and β cells. *Endocrinology.* 117:806–816.

36. Gopel, S., Q. Zhang, L. Eliasson, X. S. Ma, J. Galvanovskis, T. Kanno, A. Salehi, and P. Rorsman. 2004. Capacitance measurements of exocytosis in mouse pancreatic α-, β- and δ-cells within intact islets of Langerhans. *J. Physiol.* 556:711–726.

37. Rocheleau, J. V., W. S. Head, and D. W. Piston. 2004. Quantitative NAD(P)H/flavoprotein autofluorescence imaging reveals metabolic mechanisms of pancreatic islet pyruvate response. *J. Biol. Chem.* 279: 31780–31787.

38. Antoine, M. H., P. Lebrun, and A. Herchuelz. 1997. Cell culture conditions influence glucose-induced $[Ca^{2+}]_i$ responses in isolated rat pancreatic B cells. *Adv. Exp. Med. Biol.* 426:227–230.

39. Gilon, P., J. C. Jonas, and J. C. Henquin. 1994. Culture duration and conditions affect the oscillations of cytoplasmic calcium concentra-tion induced by glucose in mouse pancreatic islets. *Diabetologia.* 37: 1007–1014.

40. Gonzalez, A., M. P. Granados, G. M. Salido, and J. A. Pariente. 2003. Changes in mitochondrial activity evoked by cholecystokinin in isolated mouse pancreatic acinar cells. *Cell. Signal.* 15:1039–1048.

41. Duchen, M. R., P. A. Smith, and F. M. Ashcroft. 1993. Substrate-dependent changes in mitochondrial function, intracellular free calcium concentration and membrane channels in pancreatic β-cells. *Biochem. J.* 294:35–42.

42. Hope, K. M., P. O. Tran, H. Zhou, E. Oseid, E. Leroy, and R. P. Robertson. 2004. Regulation of α-cell function by the β-cell in isolated

human and rat islets deprived of glucose: the ''switch-off'' hypothesis. *Diabetes.* 53:1488–1495.

43. Ishihara, H., P. Maechler, A. Gjinovci, P. L. Herrera, and C. B. Wollheim. 2003. Islet β-cell secretion determines glucagon release from neighbouring α-cells. *Nat. Cell Biol.* 5:330–335.

44. Wendt, A., B. Birnir, K. Buschard, J. Gromada, A. Salehi, S. Sewing, P. Rorsman, and M. Braun. 2004. Glucose inhibition of glucagon secretion from rat α-cells is mediated by GABA released from neighboring β-cells. *Diabetes.* 53:1038–1045.

45. Barg, S., J. Galvanovskis, S. O. Gopel, P. Rorsman, and L. Eliasson. 2000. Tight coupling between electrical activity and exocytosis in mouse glucagon-secreting α-cells. *Diabetes.* 49:1500–1510.

46. Ravier, M. A., and G. A. Rutter. 2005. Glucose or insulin, but not zinc ions, inhibit glucagon secretion from mouse pancreatic α-cells. *Diabetes.* 54:1789–1797.

47. Ashcroft, F. M. 2000. The Yin and Yang of the K_{ATP} channel. *J. Physiol.* 528:405.

48. Schuit, F., A. De Vos, S. Farfari, K. Moens, D. Pipeleers, T. Brun, and M. Prentki. 1997. Metabolic fate of glucose in purified islet cells. Glucose-regulated anaplerosis in β cells. *J. Biol. Chem.* 272:18572–18579.

49. Heimberg, H., A. De Vos, K. Moens, E. Quartier, L. Bouwens, D. Pipeleers, E. Van Schaftingen, O. Madsen, and F. Schuit. 1996. The glucose sensor protein glucokinase is expressed in glucagon-producing α-cells. *Proc. Natl. Acad. Sci. USA.* 93:7036–7041.

50. Yamada, K., M. Nakata, N. Horimoto, M. Saito, H. Matsuoka, and N. Inagaki. 2000. Measurement of glucose uptake and intracellular calcium concentration in single, living pancreatic β-cells. *J. Biol. Chem.* 275:22278–22283.

51. Bai, L., X. Zhang, and F. K. Ghishan. 2003. Characterization of vesicular glutamate transporter in pancreatic α - and β -cells and its regulation by glucose. *Am. J. Physiol. Gastrointest. Liver Physiol.* 284: G808–G814.

52. Wang, J., Y. Cao, and D. F. Steiner. 2003. Regulation of proglucagon transcription by activated transcription factor (ATF) 3 and a novel isoform, ATF3b, through the cAMP-response element/ATF site of the proglucagon gene promoter. *J. Biol. Chem.* 278:32899–32904.

53. Fujitani, S., T. Ikenoue, M. Akiyoshi, T. Maki, and T. Yada. 1996. Somatostatin and insulin secretion due to common mechanisms by a new hypoglycemic agent, A-4166, in perfused rat pancreas. *Metabolism.* 45:184–189.

54. Efendic, S., F. Enzmann, A. Nylen, K. Uvnas-Wallensten, and R. Luft. 1979. Effect of glucose/sulfonylurea interaction on release of insulin, glucagon, and somatostatin from isolated perfused rat pancreas. *Proc. Natl. Acad. Sci. USA.* 76:5901–5904.

55. Melroe, G. T., M. M. Ehrman, J. D. Kittilson, and M. A. Sheridan. 2000. Glucose regulates pancreatic preprosomatostatin I expression. *FEBS Lett.* 465:115–118.